Journal of Rock Mechanics and Geotechnical Engineering 8 (2016) 928–935

Contents lists available at ScienceDirect

Journal of Rock Mechanics and Geotechnical Engineering

journal homepage: www.rockgeotech.org

Full Length Article

Carbon capture and storage, geomechanics and induced seismic activity

James P. Verdon*, Anna L. Stork

School of Earth Sciences, University of Bristol, Wills Memorial Building, Queen's Road, Bristol, BS8 1RJ, UK

ARTICLE INFO

Article history:
Received 31 March 2016
Received in revised form
13 June 2016
Accepted 16 June 2016
Available online 8 September 2016

Keywords:
Carbon capture and storage (CCS)
Induced seismicity
Geomechanics

ABSTRACT

Injection of large volumes of carbon dioxide (CO_2) for the purposes of greenhouse-gas emissions reduction has the potential to induce earthquakes. Operators of proposed projects must therefore take steps to reduce the risks posed by this induced seismicity. In this paper, we examine the causes of injection-induced seismicity (IIS), and how it should be monitored and modelled, and thereby mitigated. Many IIS case studies are found where fluids are injected into layers that are in close proximity to crystalline basement rocks. We investigate this issue further by comparing injection and seismicity in two areas where oilfield wastewater is injected in significant volumes: Oklahoma, where fluids are injected into a basal layer, and Saskatchewan, where fluids are injected into a much shallower layer. We suggest that the different induced seismicity responses in these two areas are at least in part due to these different injection depths. We go on to outline two different approaches for modelling IIS: a statistics based approach and a physical, numerical modelling based approach. Both modelling types have advantages and disadvantages, but share a need to be calibrated with good quality seismic monitoring data if they are to be used with any degree of reliability. We therefore encourage the use of seismic monitoring networks at all future carbon capture and storage (CCS) sites.

1. Introduction

Carbon dioxide (CO_2), produced from the burning of fossil fuels in thermal power stations and other large industrial facilities, can be captured and removed from a plant's exhaust gases. The captured CO_2 can then be transported to a sedimentary basin, and injected into a suitable geologic formation, where it is permanently trapped. This carbon capture and storage (CCS) technology has the potential to substantially reduce the greenhouse-gas emissions from fossil fuel usage.

By allowing continued fossil fuel use while mitigating emissions, CCS is vital in reducing the costs of decarbonisation. The International Energy Agency (Levina et al., 2013) has estimated that, if CCS is not used in the electricity generation sector, the capital investment needed to meet the same emissions constraints is increased by 40%. Moreover, CCS is often the only technology capable of mitigating emissions from other CO_2-intensive sources such as the cement, steel and refining industries.

Broadly speaking, research on CCS is divided between "capture" and "storage". The capture side focuses on how CO_2 is captured from the exhaust stream of a power plant (or cement factory, oil refinery, etc.): from a financial perspective, this is the costliest part of the CCS process (e.g. Nauclér et al., 2008). The storage side focuses on how CO_2 can be injected and stored in sedimentary formations. It is in understanding how the CO_2 will interact with the subsurface, and in ensuring that the injected CO_2 cannot return to the surface, that the most significant uncertainties associated with CCS are found.

Most early research on CO_2 storage was primarily concerned with the possibility that the buoyant CO_2 would move through the caprock, and eventually leak at the surface. While the fact that subsurface injection could trigger seismicity has been known for decades (e.g. Raleigh et al., 1976), the risks of CCS-induced seismicity were generally downplayed in early CCS papers (e.g. Damen et al., 2006). This was probably because induced seismicity in wider oilfield operations was relatively uncommon.

However, in recent years, a substantial increase in injected wastewater volumes in the mid-continental USA has been linked

* Corresponding author.
E-mail address: James.Verdon@bristol.ac.uk (J.P. Verdon).
Peer review under responsibility of Institute of Rock and Soil Mechanics, Chinese Academy of Sciences.

http://dx.doi.org/10.1016/j.jrmge.2016.06.004

to a dramatic increase in the number of recorded earthquakes (e.g. Ellsworth, 2013), and similar observations have been made in some Canadian basins (e.g. BC Oil and Gas Commission, 2014), and during wastewater disposal in Chinese gas fields (Lei et al., 2008, 2013). Seismic activity also appears to have been triggered by natural gas injection for storage purposes (e.g. Cesca et al., 2014). Given that the proposed injection volumes for commercial-scale CCS sites significantly exceeds the volumes injected at many of these case examples (e.g. Verdon, 2014), the risk of injection-induced seismicity (IIS) at CCS sites is being re-appraised (e.g. Zoback and Gorelick, 2012, 2015; Verdon et al., 2013; Verdon, 2014).

At present, there are still very few active commercial-scale (~1 Mt/year or more of CO_2 injected) CCS projects. Given that the geomechanical effects of subsurface injection are generally assumed to be scale-dependent (e.g. Verdon et al., 2013), the lack of commercial-scale projects means that there are as yet few opportunities to study the geomechanical impacts of large-scale CO_2 injection directly. Instead, the nascent CCS industry should look to learn from other similar industries. Most notably, there are many similarities between CCS and wastewater disposal (e.g. Verdon, 2014), and we believe that the CCS industry should examine past cases of wastewater disposal-induced seismicity in order to learn lessons that can be applied to future CCS projects.

In this paper, we begin by reviewing case examples where wastewater disposal has triggered seismicity, with the particular aim of establishing the mechanisms for induced seismicity, and the factors that might make an area prone to (or not prone to) induced seismicity. Of particular interest is the link between injection and basement rocks. We go to consider how seismicity can be modelled: we outline two different modelling approaches, one statistical and one numerical, that can be used to estimate the likely largest event size that might be triggered by an injection project. We have applied these models to the induced seismicity recorded at the In Salah CCS project, Algeria. Finally, we make recommendations for the monitoring of induced seismicity at future CCS sites.

2. Case examples of injection-induced seismicity

2.1. Mechanisms for injection-induced seismicity

The first well-recorded example of seismic activity induced by injection occurred at the Rocky Mountain Arsenal, Denver (Healy et al., 1968). The link between injection and seismicity was conclusively demonstrated in the Rangely oilfield, Colorado (Raleigh et al., 1976), where variations in injection rates and pressures produced variations in seismicity.

It is generally accepted that injection-induced seismicity occurs on pre-existing faults. A fault can slide if the shear stress on the fault, τ, exceeds the Mohr–Coulomb failure envelope:

$$\tau > \mu(\sigma_n - P) + \tau_O \quad (1)$$

where μ is the coefficient of friction, σ_n is the normal stress acting on the fault, P is the pore pressure within the fault, and τ_O is the cohesive strength of the fault surface. Subsurface injection can thereby lead to seismicity if it leads to either shear stress increases, normal stress decreases, or pore pressure increases, on a fault. This can happen in a number of ways:

- When fluids are injected, pore pressures will inevitably increase to accommodate the additional volumes in the subsurface. This pore pressure increase is the most direct way that injection can lead to seismicity.
- Injection may also cause an expansion of the reservoir, which will alter the stress field in the rocks surrounding the reservoir, potentially leading to fault slip outside the reservoir.
- Once faults begin to slip, the displacement along a fault will create further stress changes capable of triggering events (e.g. King et al., 1994).

Several of these mechanisms may act together during a sequence of induced events. For example, Sumy et al. (2014) studied the seismicity triggered by wastewater disposal near to Prague, Oklahoma, finding that the initial events were likely to have been caused by pore pressure increases in the reservoir, but those subsequent events were triggered by static stress transfer generated by slip along the re-activated fault. It is often challenging to determine precisely the causative mechanism for a series of triggered events (e.g. Cesca et al., 2014).

2.2. Induced seismicity in sediments and basement rocks

Verdon (2014) examined a selection of IIS case studies (all induced by wastewater disposal), and found that seismicity tends to occur at depths below the injection interval, and indeed in many cases, most of the events are observed in the crystalline basement that underlies the sedimentary basin (Fig. 1). Vilarrasa and Carrera (2015) suggested that this is because deviatoric stresses tend to be higher in basement rocks compared to the overlying sediments. Vilarrasa and Carrera (2015) went on to conclude that IIS during CO_2 injection was therefore unlikely.

The relationship between injection into near-basement rocks and IIS merits further consideration. In many IIS case examples, fluids are injected into sedimentary layers that are in close proximity to the crystalline basement. For example, in Oklahoma, where a significant increase in IIS has been observed, much of the injection is into the basal Arbuckle Formation, which directly overlies the pre-Cambrian basement. Similarly, injection into the basal Mt Simon Formation in Ohio and Illinois has led to cases of IIS (e.g. Nicholson et al., 1988; Seeber et al., 2004), including at the Decatur CO_2 injection pilot project (Kaven et al., 2015).

Verdon et al. (2016) compared induced seismicity in two areas that have seen extensive hydrocarbon-extraction-related activity over many decades: Oklahoma, and southeast Saskatchewan. In

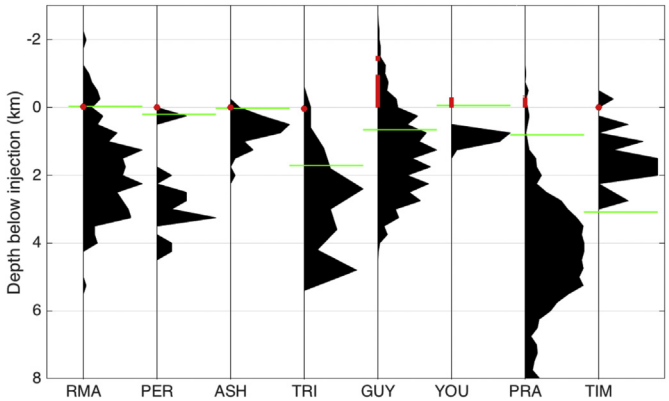

Fig. 1. Histograms showing event depths at various IIS case studies relative to the deepest injection depth. Modified from Verdon (2014). The red lines mark the injection intervals at each site, and the green lines mark the approximate position of the crystalline basement. The case studies considered are: RMA = Rocky Mountain Arsenal (Healy et al., 1968); PER = Perry, Ohio (Nicholson et al., 1988); ASH = Ashtabula, Ohio (Seeber et al., 2004); TRI = Trinidad, Colorado (Meremonte et al., 2002); GUY = Guy, Arkansas (Horton, 2012); YOU = Youngstown, Ohio (Kim, 2013); PRA = Prague, Oklahoma (Keranen et al., 2013); and TIM = Timpson, Texas (Frohlich et al., 2014).

both areas, conventional fields have been active for a long time, there are high-volume wastewater disposal wells present, and hydraulic fracturing is used to extract unconventional resources. In Fig. 2, we compare the numbers of high-volume injection wells in both regions (normalised by the respective study areas) and we note that the number of wells and their maximum monthly injection rates are similar. However, while injection well volumes are similar, Oklahoma has seen a substantial increase in seismicity, related primarily to high-volume disposal wells, while almost no oilfield-related seismicity has been detected in Saskatchewan.

One potential reason for the difference in IIS between the two areas is that stress conditions in Saskatchewan are such that faults are less likely to rupture. However, a substantial number of earthquakes have been identified in southeast Saskatchewan that are associated with potash mining. Stress conditions in the area must be such that seismicity can be induced given the appropriate forcing.

One key difference between these two areas is the different geological units used for wastewater disposal. As stated above, most of the wastewater disposal in Oklahoma is into the Arbuckle Formation, which is a basal formation that directly overlies, and therefore is likely to be hydraulically connected to, the crystalline basement. This means that pore pressure increases in this layer can be easily communicated into the underlying basement rocks.

In contrast, in southeast Saskatchewan, the only sedimentary formations that experience a net volume increase are Cretaceous formations, and there is significant separation (usually several kilometres) between these units and the pre-Cambrian crystalline basement. Verdon et al. (2016) surmised that this difference in injection strategy – targeting shallower aquifers rather than basal formations – may account for the very different IIS responses between the two regions.

With respect to CO_2 leakage, deeper formations have generally thought to be a better option, because there is more stratigraphy through which CO_2 would have to leak before it reaches the surface. However, on this understanding, with respect to IIS, deeper formations may in fact pose a higher risk if they are hydraulically connected to the crystalline basement.

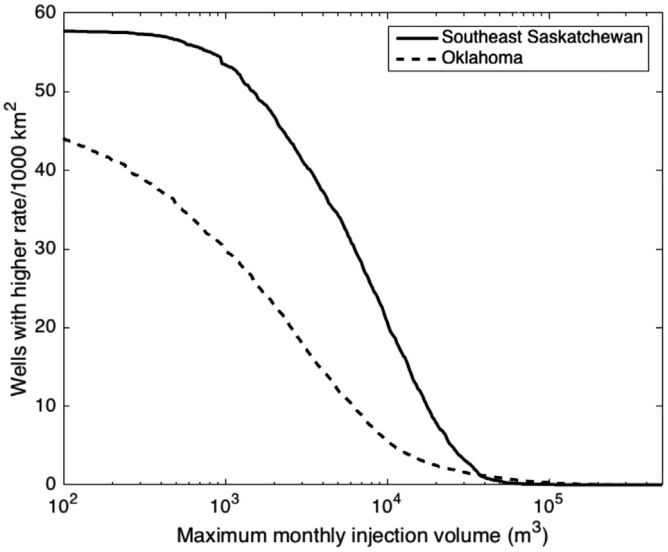

Fig. 2. Number of wells as a function of their highest monthly injection volume for southeast Saskatchewan (Verdon et al., 2016) and Oklahoma, normalised by the respective study areas. Overall, Saskatchewan has more injection wells, but the number of high-volume wells per unit area is similar.

However, our assessment does not conclude that, so long as basal sedimentary layers are avoided, then IIS can be completely mitigated, as suggested by Vilarrasa and Carrera (2015). Evidently, there are cases where injection into shallower layers, that have significant separation from the basement, has produced IIS, including at Trinidad, Colorado (Meremonte et al., 2002), Timpson, Texas (Frohlich et al., 2014), and at the In Salah CCS demonstration project (Stork et al., 2015). In Chinese gas fields, seismicity has been observed both in basement rocks (Lei et al., 2008) at some sites, but also contained entirely within overlying sedimentary formations (Lei et al., 2013) at others. Clearly, sedimentary formations are capable of supporting sufficient deviatoric stresses on faults such that IIS can be generated without a direct hydraulic connection to the crystalline basement (e.g. Zoback and Gorelick, 2015).

3. Modelling seismicity

If the risks of IIS are to be mitigated, then we must develop models capable of simulating IIS at proposed sites. This will allow operators to identify sites at which IIS might become an issue, and to moderate the CO_2 injection programme such that the risk is reduced. Broadly speaking, models for IIS fall into two types: statistical models, which use recorded events during the early stages of operation to forecast what will occur as injection continues; and physical models, which numerically simulate the processes occurring in a reservoir. In the following sections, we demonstrate each type of model, as applied to the In Salah CCS project, Algeria, and discuss the strengths and weaknesses of each model type.

3.1. CO_2 injection and seismicity at the In Salah CCS project

Between 2004 and 2011, over 3.8 million tonnes of CO_2 were injected via three injection wells into the water leg of a natural gas reservoir at In Salah, Algeria. The CO_2 had been stripped from the producing wells of several nearby gas fields. The CO_2 storage operation is summarised in Fig. 3. The reservoir consisted of a 20 m thick Carboniferous sandstone, overlain by approximately 950 m of mudstone rocks that acted as a caprock. The reservoir had relatively low porosity (13%–20%) and permeability (averaging 10 mD), meaning that injection led to substantial pore pressure increases, which in turn produced significant amounts of geomechanical deformation. This deformation was first identified using InSAR methods (Onuma and Ohkawa, 2009).

In 2009, a monitoring network was installed near to one of the three injection wells (KB-502, labelled in Fig. 3). A string of geophones was installed in a shallow borehole at the depth of 80–500 m. However, technical issues with the deployment meant that fully-useable data were available only from the uppermost instrument. Nevertheless, Stork et al. (2015) identified P- and S-wave picks for over 6000 events between August 2009 and June 2011. Stork et al. (2015) computed moment magnitudes for these events, finding that the largest event had a magnitude of 1.7. More details regarding the event positions, occurrence rates and frequency–magnitude distributions of the observed events are available in Stork et al. (2015) and Verdon et al. (2015). It is these observed events, and especially their largest magnitudes, that we focus on modelling here, using both statistical and numerical methods.

3.2. Statistical model

McGarr (2014) identified that the cumulative seismic moment released during injection, ΣM_O, could be scaled with the injection volume, ΔV:

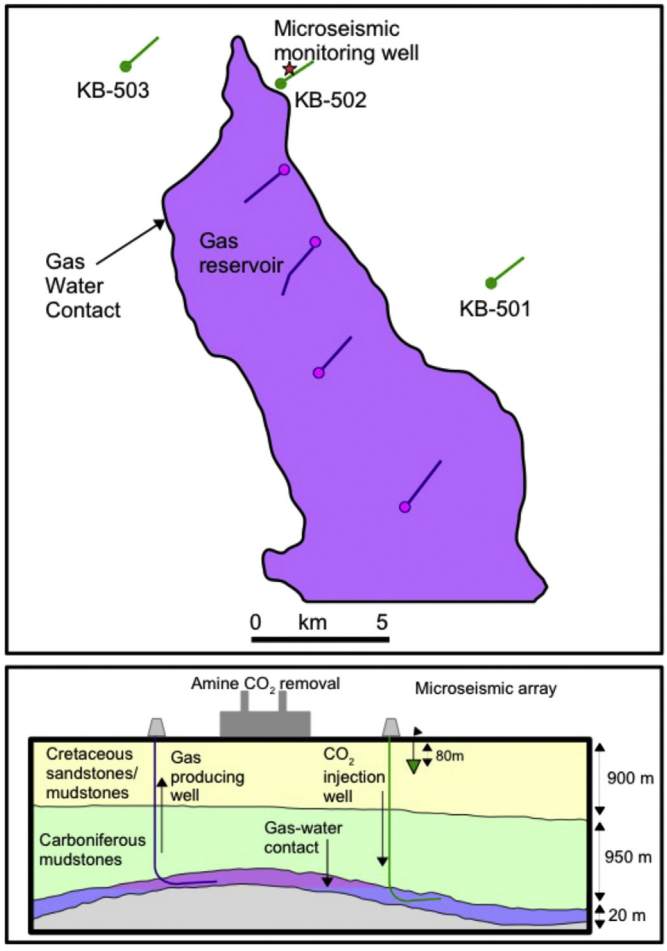

Fig. 3. Schematic diagram summarising CCS operations at In Salah. Gas is produced from a sandstone reservoir at the centre of an anticline formation. CO_2 is stripped from this gas stream and re-injected into the water leg of the same formation.

$$\Sigma M_O = G\Delta V \tag{2}$$

where G is the rock shear modulus. This relationship applies to situations where almost all of the deformation induced by injection is released seismically. However, in most cases, much or all of the deformation may occur aseismically, meaning that the ΣM_O falls well below this value. Hallo et al. (2014) therefore suggested a modification to Eq. (2), introducing a "seismic efficiency" term S_{EFF}:

$$\Sigma M_O = S_{EFF} G\Delta V \tag{3}$$

If seismic activity is closely monitored from the start of injection, then S_{EFF} can be quickly and easily determined from the observed moment release, and the known injection volume. Given that an operator will have a planned total injection volume, then if it is assumed that S_{EFF} does not change during injection, the total seismic moment release during the life of the project can be determined from Eq. (3).

Given an expected cumulative moment, the magnitude of the largest event, M_{MAX}, is determined by the Gutenberg–Richter b value. Much like S_{EFF}, the b value can be easily determined if a site is well-monitored. From the measured b value and S_{EFF}, the expected value for M_{MAX} can be computed using the equations of Hallo et al. (2014):

$$\Sigma M_O = 10^{9.1}\frac{10^a b}{1.5-b}\left[10^{M_{MAX}(1.5-b)} - 10^{M_{MIN}(1.5-b)}\right] \tag{4}$$

where

$$a = bM_{MAX} - \log_{10}\left(10^{b\delta} - 10^{-b\delta}\right) \tag{5}$$

where M_{MIN} is the completeness magnitude defined when calculating the b value, and δ is the probabilistic half-bin size defined around M_{MAX} as described by Hallo et al. (2014).

The results for In Salah are shown in Fig. 4. In the lower panel, we continually update b and S_{EFF} based on the observed events. In the upper panel, we forecast M_{MAX} based on these values and Eq. (4). The largest event to be recorded at In Salah had a magnitude of 1.7 (Stork et al., 2015). We note that, based only on the smaller events observed during the early stages of monitoring, we are able to forecast the magnitude of this largest event.

3.3. Physical, numerical model

As an alternative to statistical methods, numerical models can be used to simulate the physical processes occurring in a reservoir, including slip on pre-existing faults. We assume that all IISs occur on pre-existing faults and fractures. The basis of our modelling approach, outlined in detail in Verdon et al. (2015), is that if we know or can simulate the positions, orientations and sizes of fractures in the reservoir, and if we can simulate both the initial stress conditions at the start of injection, and the changes in stress during injection, then we can identify when and where fractures exceed the Mohr–Coulomb failure envelope (Eq. (1)), generating seismicity.

The simulated fracture network for In Salah was generated using a geo-structural model described by Bond et al. (2013). The faulted, folded reservoir was reconstructed from the original, flat-lying sedimentary layers using a mass-spring solver. Doing so creates a map of strain intensity and orientation throughout the reservoir. Bond et al. (2013) used these strain maps to populate a modelled fracture network. Two fracture sets were generated, one associated with faulting, and the other associated with folding. In total, the

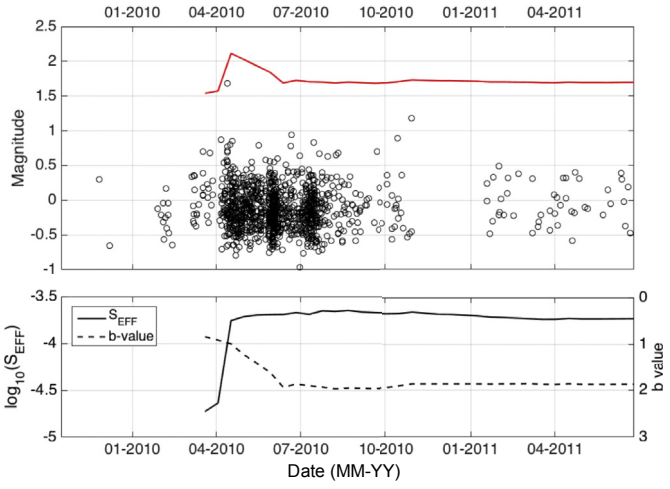

Fig. 4. Using a statistical method to forecast M_{MAX} during CO_2 injection at In Salah. In the lower panel, b values (dashed line) and seismic efficiency (solid line) are continually updated during injection. In the upper panel, Eq. (4) is used to forecast M_{MAX} (red line). Also plotted are the observed event magnitudes (black dots). The largest observed event has a magnitude of 1.7. Based on the M_{MAX} forecast from the early events, an event of this size is expected.

position, orientation and length of over 300,000 fractures were modelled.

The initial stress conditions and the pore pressure changes during injection (from which effective stress changes were computed) were simulated using a history-matched, finite element coupled flow/geomechanical reservoir model (Bissell et al., 2011). The model consisted of 1.7 million grid cells (133 × 188 × 69), and simulated an area of 40 km × 40 km laterally, centred on the CO_2 injection wells, to a depth of 3.5 km.

The stress field acting on each modelled fracture is based on the stress conditions at the nearest node of the geomechanical model. However, to account for natural variability in the subsurface, the principal stress magnitudes are modulated by a factor randomly chosen from a normal distribution with mean 0% and standard deviation 10%, before being rotated by Euler angles chosen at random from a normal distribution with mean 0° and standard deviation 5°.

We resolve the normal (σ_n) and shear (τ) stresses acting on each fracture using the modelled effective stress, σ^e_{ij}:

$$\left.\begin{aligned} -t &= \sigma^e_{ij}\boldsymbol{n} \\ -\sigma_n &= (t\cdot\boldsymbol{n})\boldsymbol{n} \\ -\tau &= t-\sigma_n \end{aligned}\right\} \quad (6)$$

where $\boldsymbol{n}$ is a unit vector normal to the fracture face. To determine whether or not a fracture will slip, producing a seismic event, Mohr–Coulomb properties for each fracture are also assigned at random from statistical populations: cohesion is selected from a normal distribution with a mean of 2.2 MPa and a standard deviation of 0.5 MPa, and the coefficient of friction from a normal distribution with a mean of 0.6 and a standard deviation of 0.1. If, for a given fracture, Eq. (1) is exceeded, then a seismic event is triggered.

The moment release, and thereby the magnitude, of the resulting event can be determined from the rupture area, A, and the stress drop, $\Delta\sigma$:

$$M_O = \Delta\sigma A^{1.5} \quad (7)$$

The stress drop is taken as the value of shear stress at the time of failure, modulated by a factor chosen at random from a uniform distribution of 1%–100%. The fracture area is computed from the fracture length, multiplied by the thickness of the reservoir (20 m). The rupture area is taken as the fracture area modulated by a random factor of 1%–100%. These modulation factors account for the fact that seismic events may not rupture the entirety of the fracture plane on which they occur, nor will they necessarily release all of the shear stress acting on them.

After an event occurs, the stress on a fracture that has slipped will be reduced, making further slip less likely. This is accounted for in our simulations: for fractures where an event has occurred, the shear stress at subsequent time-steps is reduced by subtracting the stress drop released in the previous events.

Fig. 5 compares the observed rate of seismicity at In Salah, and that reproduced by our model. Our model provides a decent match with the observations, with the increased injection rates and pressures in summer 2010 leading to a substantial increase in seismic activity, which reduces once the rates are reduced in the later part of 2010.

Fig. 6 compares the observed and modelled frequency-magnitude distributions. With respect to the largest magnitudes, our modelled value for $M_{MAX} = 1.73 \pm 0.1$, which is in good agreement with the observed largest event, which had a magnitude

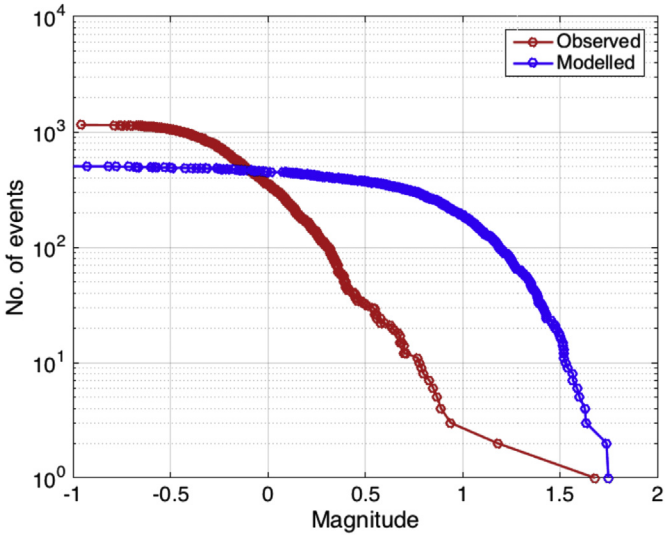

Fig. 6. Comparison of observed (red) and numerically modelled (blue) event frequency-magnitude distributions for In Salah. The modelled and observed largest events have similar magnitudes, but there are more small events in the observed population than those reproduced by the model.

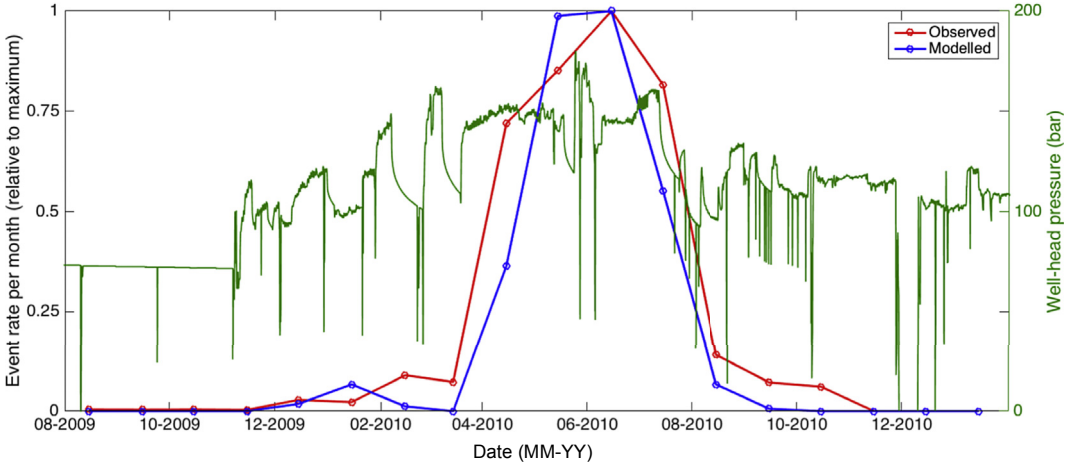

Fig. 5. Comparison of the relative monthly event rate between the observed events (red) and the modelled population (blue), scaled relative to the maximum monthly rates. A good match between model and observation is obtained. Also shown is the injection pressure in well KB-502 (green). 1 bar = 100 kPa.

of 1.7. The simulated magnitudes are derived from the modelled stress drop and fracture size. That our modelled value for M_{MAX} matches the observed value implies that our modelling was able to accurately constrain both the stress conditions in the reservoir, and the fracture-length distribution.

The most significant discrepancy between our model and the observed events is the relative paucity of smaller events produced by our model in comparison to reality. This discrepancy was discussed at length in Verdon et al. (2015), who considered a number of potential contributing factors, including: the Mohr–Coulomb properties of the fractures; the temporal resolution of the modelling; stress interactions between fractures (which are neglected in this modelling approach); the creation of additional fractures by hydraulic fracturing (only shear events are considered in this approach); and fracturing outside of the reservoir zone.

Verdon et al. (2015) concluded that the most likely reason for the discrepancy is length distribution of fractures in the model. The fracture model was originally created to simulate fluid flow (Bond et al., 2013), not seismicity, and the smallest simulated fracture length was 50 m. By simulating a larger number of smaller fractures, and fewer intermediate-sized fractures, the mismatch between observed and modelled event distributions might be reduced substantially.

3.4. Comparison between statistical and numerical models

In the above examples, both the physical and statistical models did a reasonable job of matching the observed IIS. The statistical model does not require any geological information in its use (this may be considered a good or a bad thing, depending on your background!). The major advantage is that it is easy to use. With robust monitoring at a CCS site, both the seismic efficiency and the b value can be easily computed, and the resulting forecast for M_{MAX} is easily obtained as a result.

However, the major assumption is that both b and S_{EFF} will remain constant throughout the injection period. It is by no means certain that this will always be the case. As injection continues, the volume of rock affected by the injection-induced pressure increase will widen. It may therefore begin to impinge on different geological structures, such as faults, that were not previously being affected, leading to a change in either b or S_{EFF} or both. Nevertheless, with robust, near-real-time monitoring, these changes could be identified prior to the triggering of the largest events, potentially allowing this risk to be mitigated.

In contrast, the physical model we have presented requires a significant quantity of geological information to be provided. As with any physical model, the results will only be as good as the data used as input. The input data used here (the geo-structural fracture model, the history-matched flow/geomechanical simulation) were themselves the fruits of extensive work programmes conducted at considerable expense both in terms of manpower and computational power. These models were themselves developed from extensive geological characterisation programmes, including from well logs, three-dimensional (3D) reflection seismic imaging, rock physics properties from laboratory testing, and InSAR imaging of surface deformation. This gives an indication of the scale of work that may be needed at future sites to ensure that CO_2 can be stored safely.

3.5. On the need for robust monitoring

One of the reasons that causative mechanisms of IIS are not well constrained is that seismic monitoring networks are not commonly deployed at injection sites. In many well-known case examples (e.g. Keranen et al., 2013; Clarke et al., 2014), monitoring networks have been deployed only after large events were triggered, meaning that data are not available to try to understand the processes that occurred during the onset of triggering.

Whether statistical or numerical models are used to simulate IIS, robust monitoring is needed if they are to be used effectively. For obvious reasons, statistical models are more effective when a larger number of events are used to calculate b and S_{EFF}. The better quality monitoring array used, the lower the detection threshold, and therefore the more events that might be available for analysis.

Physical models use a wide range of input parameters. Often, these parameters are not completely constrained, leaving parameters available to be "tuned". In order to have confidence that numerical models are providing a reasonable representation of reality, model forecasts should be compared with field observations. There are a number of geophysical observations that can be used to calibrate geomechanical models, including four-dimensional (4D) seismic reflection imaging, and measurements of surface displacement made by GPS or InSAR. However, the most obvious observation to be used when calibrating a geomechanical model used to simulate IIS is microseismic activity induced by injection. The better the quality of data collected during injection, the more effectively a geomechanical model can be calibrated.

Options for seismic monitoring arrays vary. The simplest and cheapest solution is generally to install an array of 5–15 surface monitoring stations around the injection site. Depending on noise conditions, such an array will be able to detect events down to $M = -1$. Such events might be used to identify the risks of induced larger seismic events, but may not be sufficient to image the detailed geomechanical response of the reservoir.

By placing instruments downhole in wells near to the reservoir, detection thresholds can be reduced substantially (to $M = -3$ or smaller, depending on noise conditions). Doing so is generally more expensive than a surface-based array. However, such events can be used to image the geomechanical response of the reservoir to injection (e.g. Verdon et al., 2011), as well as to assess the likelihood of larger, felt seismic events being triggered as injection continues (e.g. Verdon, 2016). Such microseismic monitoring arrays may also detect events in the caprock, which in some cases may be indicative of upward fluid migration. However, Verdon (2016) has shown that microseismicity in the caprock can also be caused by stress transfer into the overburden, without any hydraulic connection. Therefore, care must be taken when interpreting microseismic observations, as interpretations may differ on a site-by-site bases (e.g. Verdon et al., 2013).

The use of seismic monitoring at pilot CCS projects has been mixed. We summarise its use at some significant CCS projects below:

Weyburn: A downhole microseismic monitoring array was installed to cover a small portion of the field. Approximately 200 events were recorded over a 6-year period, all with magnitudes less than 0. Verdon et al. (2011) used these events to constrain geomechanical models of the field.

Sleipner: No seismic monitoring has been used at Sleipner. Therefore, it is impossible to rule out that small-scale seismicity has happened. However, because the Utsira Sandstone storage reservoir is very large and porous, injection has caused only very small pressure increases, which makes IIS less likely (Verdon et al., 2013).

Snøhvit: Much like Sleipner, no seismic monitoring has been used at Snøhvit. However, unlike Sleipner, pore pressures increased substantially during the initial injection phase into the Tubåen Formation, which necessitated a change in injection strategy, using the shallower Stø Formation instead. It is not

known whether the pore pressure increases in the Tubåen Formation had any geomechanical impacts.

In Salah: As discussed in previous sections, seismic monitoring was installed at In Salah, but only after 5 years of injection had taken place, and significant geomechanical impacts had been observed by other methods. The monitoring array consisted of a single geophone in a shallow borehole. Over 6000 events were detected during the monitoring period, the largest of which had a magnitude of 1.7.

Aquistore: A monitoring array of 65 geophones has been deployed to monitor microseismicity at the Aquistore site. These geophones are buried to depths of 5–20 m, and form part of a larger network that was deployed primarily for repeat seismic reflection surveys. No microseismic events have been detected, although only a small portion of the planned injection volume has yet been stored.

Cranfield: A seismic monitoring array was deployed consisting of six instruments buried in shallow boreholes 100 m deep. No seismic events have been detected (Hovorka et al., 2013).

Decatur: Two separate monitoring arrays were installed to monitor the Illinois Basin-Decatur Project: a downhole microseismic monitoring array consisting of 34 multicomponent geophones in two deep boreholes (Bauer et al., 2016), and a secondary array consisting of 13 broadband seismic instruments at the surface and 4 accelerometers deployed in 150 m-deep boreholes (Kaven et al., 2015). The downhole microseismic array detected a total of 4747 events during 3 years of CO_2 injection, with an average magnitude of −0.9. The surface monitoring array has detected 179 events, with magnitudes ranging from −1.1 to 1.3.

Aneth: A downhole array of 60 geophones was deployed to monitor CO_2-EOR at the Aneth Field. Produced water from the field was also being injected into an underlying aquifer. No seismicity was detected associated with the CO_2 injection, but the underlying produced water disposal generated approximately 1400 events over the course of 1 year, with the largest event having a magnitude of 1.2 (Rutledge, 2010).

Lacq-Rousse: A hybrid seismic monitoring array was installed to monitor CO_2 storage at the Lacq-Rousse field, consisting of 1 surface seismometer, 7 shallow arrays of 4 geophones each buried to depths of approximately 200 m, and a deep downhole array of 3 accelerometers. This system detected over 2500 reservoir-related microseismic events over 3 years of monitoring, all of which had magnitudes less than 0 (Payre et al., 2014).

4. Conclusions

Injection of CO_2 into subsurface reservoirs has the potential to trigger seismicity. Therefore, the risks posed by IIS must be considered at all future CCS sites. We can also learn much by studying past incidents of IIS in other industries, such as the shale gas, wastewater disposal and hydraulic fracturing industries. In many such case studies, IIS has been associated with injection into layers that have a potential hydraulic connection to the underlying crystalline basement.

Previously, such layers have been considered optimal targets for CCS, because their greater depth means a larger distance for CO_2 to migrate back to the surface in the event of leakage. However, if near-basement injection poses a greater seismic hazard, then such considerations may have to be revised, and injection targets chosen that do not have a hydraulic connection to the crystalline basement. However, it should be noted that avoiding near-basement layers alone is not a sufficient condition to avoid IIS.

The hazards posed by IIS can be mitigated by effective modelling and monitoring regimes. We have demonstrated two types of modelling approaches – statistical and numerical. The statistical approach uses the characteristics of smaller event populations recorded during the early stages of injection to make forecasts about what will happen as injection volumes increase. The numerical approach involves building a geomechanical simulation that models how injection will alter the stress conditions on pre-existing faults and fractures in the reservoir.

We have applied both models to the seismicity recorded during CO_2 injection at the In Salah CCS project. Both models were able to successfully simulate the magnitude of the largest recorded event. Each modelling type has benefits and disadvantages. The statistical model is relatively simple and easy to use, but requires as an assumption that both the amount of seismicity induced per unit volume injected and the *b* value remain constant during injection, which may not be the case. The numerical model requires an extensive geological characterisation programme in order to provide reliable input data, and is both labour- and computationally-intensive. However, regardless of the modelling method used, good quality monitoring is required to mitigate IIS at future CCS sites.

If CCS is to make a significant impact on global CO_2 emissions, a large number of commercial-scale CCS projects will be required. Comparisons with other industries suggest that IIS at some sites will be inevitable (indeed, we have already seen low levels of IIS at multiple pilot projects). However, the risk posed by IIS during CO_2 injection must be weighted against the risks of allowing anthropogenic emissions to remain unmitigated, leading to increased climate change.

Conflict of interest

We wish to confirm that there are no known conflicts of interest associated with this publication and there has been no significant financial support for this work that could have influenced its outcome.

Acknowledgements

James Verdon's Research Fellowship at the University of Bristol is supported by the British Geological Survey. We would like to thank the operators of the In Salah JV and JIP for providing the data from In Salah shown in this paper.

References

Bauer RA, Carney M, Finley RJ. Overview of microseismic response to CO_2 injection into the Mt Simon saline reservoir at the Illinois Basin-Decatur project. International Journal of Greenhouse Gas Control 2016. http://dx.doi.org/10.1016/j.ijggc.2015.12.015 (in press).

Bissell RC, Vasco DW, Atbi M, Hamdani M, Okwelegbe M, Goldwater MH. A full field simulation of the In Salah gas production and CO_2 storage project using a coupled geomechanical and thermal fluid flow simulator. Energy Procedia 2011;4:3290–7.

Bond CE, Wightman R, Ringrose PS. The influence of fracture anisotropy on CO_2 flow. Geophysical Research Letters 2013;40(7):1284–9.

BC Oil and Gas Commission. Investigation of observed seismicity in the Montney trend. 2014.

Cesca S, Grigoli F, Heimann S, González Á, Buforn E, Maghsoudi S, Blanch E, Dahm T. The 2013 September–October seismic sequence offshore Spain: a case of seismicity triggered by gas injection? Geophysical Journal International 2014;198(2):941–53.

Clarke H, Eisner L, Styles P, Turner P. Felt seismicity associated with shale gas hydraulic fracturing: the first documented example in Europe. Geophysical Research Letters 2014;41(23):8308–14.

Damen K, Faaij A, Turkenburg W. Health, safety and environmental risks of underground CO_2 storage – overview of mechanisms and current knowledge. Climatic Change 2006;74(1):289–318.

Ellsworth W. Injection-induced earthquakes. Science 2013;341(6142). http://dx.doi.org/10.1126/science.1225942.
Frohlich C, Ellsworth W, Brown WA, Brunt M, Luetgert J, MacDonald T, Walter S. The 17 May 2012 M4.8 earthquake near Timpson, East Texas: an event possibly triggered by fluid injection. Journal of Geophysical Research 2014;119(1):581–93.
Hallo M, Oprsal I, Eisner L, Ali MY. Prediction of magnitude of the largest potentially induced seismic event. Journal of Seismology 2014;18(3):421–31.
Healy JH, Rubey WW, Griggs DT, Raleigh CB. The Denver earthquakes. Science 1968;161(3848):1301–10.
Horton S. Injection into subsurface aquifers triggers earthquake swarm in Central Arkansas with potential for damaging earthquake. Seismological Research Letters 2012;83(2):250–60.
Hovorka SD, Meckel TA, Treviño RH. Monitoring a large-volume injection at Cranfield, Mississippi – project design and recommendations. International Journal of Greenhouse Gas Control 2013;18:345–60.
Kaven JO, Hickman SH, McGarr AF, Ellsworth WL. Surface monitoring of microseismicity at the Decatur, Illinois, CO_2 sequestration demonstration site. Seismological Research Letters 2015;86(4):1096–101.
Keranen KM, Savage H, Abers GA, Cochran ES. Potentially induced earthquakes in Oklahoma, USA: links between wastewater injection and the 2011 M_W 5.7 earthquake sequence. Geology 2013;41(6):699–702.
Kim WY. Induced seismicity associated with fluid injection into a deep well in Youngstown, Ohio. Journal of Geophysical Research 2013;118(7):3506–18.
King GCP, Stein RS, Lin J. Static stress changes and the triggering of earthquakes. Bulletin of the Seismological Society of America 1994;84(3):935–53.
Lei X, Yu G, Ma S, Wen X, Wang Q. Earthquakes induced by water injection at ~3 km depth within the Rongchang gas field, Chongqing, China. Journal of Geophysical Research 2008;113(B10). http://dx.doi.org/10.1029/2008JB005604.
Lei X, Ma S, Chen W, Pang C, Zeng J, Jiang B. A detailed view of the injection-induced seismicity in a natural gas reservoir in Zigong, southwestern Sichuan Basin, China. Journal of Geophysical Research 2013;118(8):4296–311.
Levina E, Bennett S, McCoy S. Technology roadmap: carbon capture and storage. Paris, France: International Energy Agency; 2013.
McGarr A. Maximum magnitude earthquakes induced by fluid injection. Journal of Geophysical Research 2014;119(2):1008–19.
Meremonte ME, Lahr JC, Frankel AD, Dewey JW, Crone AJ, Overturf DE, Carver DL, Rice WT. Investigation of an earthquake swarm near Trinidad, Colorado, August-October 2001. U.S. Geological Survey Open-File Report 02-0073. 2002.
Nauclér T, Campbell W, Ruijs J. Carbon capture and storage: assessing the economics. McKinsey & Company; 2008.
Nicholson C, Roeloffs E, Wesson RL. The Northeastern Ohio earthquake of 31 January 1986: was it induced? Bulletin of the Seismological Society of America 1988;78(1):188–217.
Onuma T, Ohkawa S. Detection of surface deformation related with CO_2 injection by DInSAR at In Salah, Algeria. Energy Procedia 2009;1(1):2177–84.
Payre X, Maisons C, Marblé A, Thibeau S. Analysis of the passive seismic monitoring performance at the Rousse CO_2 storage demonstration pilot. Energy Procedia 2014;63:4339–57.
Raleigh CB, Healy JH, Bredehoeft JD. An experiment in earthquake control at Rangely, Colorado. Science 1976;191(4233):1230–7.
Rutledge J. Geologic demonstration at the Aneth Oil Field, Paradox Basin, Utah. Southwest Regional Partnership of Carbon Sequestration. 2010.
Seeber L, Armbruster JG, Kim WY. A fluid-injection-triggered earthquake sequence in Ashtabula, Ohio: implications for seismogenesis in stable continental regions. Bulletin of the Seismological Society of America 2004;94(1):76–87.
Stork AL, Verdon JP, Kendall JM. The microseismic response at the In Salah carbon capture and storage (CCS) site. International Journal of Greenhouse Gas Control 2015;32:159–71.
Sumy DF, Cochran ES, Keranen KM, Wei M, Abers GA. Observations of static Coulomb stress triggering of the November 2011 M5.7 Oklahoma earthquake sequence. Journal of Geophysical Research 2014;119(3):1904–23.
Verdon JP. Significance for secure CO_2 storage of earthquakes induced by injection. Environmental Research Letters 2014;9(6):064022.
Verdon JP. Using microseismic data recorded at the Weyburn CCS-EOR site to assess the likelihood of induced seismic activity. International Journal of Greenhouse Gas Control 2016. http://dx.doi.org/10.1016/j.ijggc.2016.03.018 (in press).
Verdon JP, Kendall JM, White DJ, Angus DA. Linking microseismic event observations with geomechanical models to minimise the risks of storing CO_2 in geological formations. Earth and Planetary Science Letters 2011;305(1–2):143–52.
Verdon JP, Kendall JM, Stork AL, Chadwick RA, White DJ, Bissell RC. Comparison of geomechanical deformation induced by megaton-scale CO_2 storage at Sleipner, Weyburn, and In Salah. Proceedings of the National Academy of Sciences of the USA 2013;110(30):E2762–71.
Verdon JP, Stork AL, Bissell RC, Bond CE, Werner MJ. Simulation of seismic events induced by CO_2 injection at In Salah, Algeria. Earth and Planetary Science Letters 2015;426:118–29.
Verdon JP, Kendall JM, Horleston AC, Stork AL. Subsurface fluid injection and induced seismicity in southeast Saskatchewan. International Journal of Greenhouse Gas Control 2016. http://dx.doi.org/10.1016/j.ijggc.2016.04.007 (in press).
Vilarrasa V, Carrera J. Geologic carbon storage is unlikely to trigger large earthquakes and reactivate faults through which CO_2 could leak. Proceedings of the National Academy of Sciences of the USA 2015;112(19):5938–43.
Zoback MD, Gorelick SM. Earthquake triggering and large-scale geologic storage of carbon dioxide. Proceedings of the National Academy of Sciences of the USA 2012;109(26):10164–8.
Zoback MD, Gorelick SM. To prevent earthquake triggering, pressure changes due to CO_2 injection need to be limited. Proceedings of the National Academy of Sciences of the USA 2015;112(33):E4510.

James P. Verdon received M.A. and M.Sci. degrees in Natural Sciences from Cambridge University, and completed his Ph.D. in Geophysics at the University of Bristol. For his PhD thesis he was awarded the Keith Runcorn Prize for the best doctoral thesis in geophysics by the Royal Astronomical Society. He is presently a Senior Research Fellow in the School of Earth Sciences, University of Bristol, where his position is funded by the British Geological Survey (BGS). He has published over 30 articles in peer-reviewed, scholarly publications.